Statistical Theory of Self-Interacting Elastomeric "Star" Networks: Mechanical and Scattering Properties

Clive A. Croxton

Department of Mathematics, University of Newcastle, Newcastle, NSW 2308, Australia

Received July 8, 1991; Revised Manuscript Received October 7, 1991

ABSTRACT: The iterative convolution (IC) technique for the prediction of spatial correlation within polymeric systems is extended to the description of the structural and thermodynamic properties of athermal elastomeric networks. In particular, the role of excluded volume, the specification of cross-linkage, and chain slipping at entanglements is investigated. Finally, the scattering functions from such networks are compared with experimental determinations, and the qualitative agreement is found to be good.

Introduction

The statistical mechanical description of the configurational and scattering properties of elastomeric networks has made considerable progress recently in terms of developments based on the so-called Gaussian phantom network of James and Guth.[1] Although the initial development of the theory occurred more than 40 years ago, subsequent refinement of the analysis did not occur for another 30 years. Indeed, it is only now, with the recognition of the technological status of polymeric elastomers, that both experimental and theoretical interest in networks has become widespread. In the phantom network, junctions are connected by Gaussian chains of covalent bonds, and since intermolecular interaction is totally neglected, both chains and junctions pass freely through one another subject only to the connectivity of the network. This, of course, introduces a number of important simplifications, not the least of which is the expression of the total configurational partition function of the system as the product of the partition functions for the individual chains. Developments of the phantom network theory yielding the configurational and fluctuation properties of the system have been presented by Graessley[2] and by Flory[3] and Pearson,[4] the latter of whom necessarily restricted their analyses to networks having a treelike structure, symmetrically grown about a central chain with no closed cyclical loops. Indeed, recent progress in the theoretical description of networks by Kloczkowski et al.[5] has also been restricted to networks of this particular topology, and although their developments provide an elegant description for this class of networks, alternative approaches based upon differing topologies would be useful. Noncovalent (excluded volume) interactions are also totally neglected in these treatments despite their crucial role in preventing the collapse of the network. The contributions of both the covalent "entropic spring" and the noncovalent interactions are now recognized as being of comparable magnitude.[21]

In the phantom network points along the chain contour as well as the junctions themselves fluctuate freely in time. While rendering the system mathematically tractable, the relative confinement of the junctions arising from the network connectivity and self-interaction is neglected, a feature specifically incorporated in the *affine* network. In this system the vectors linking end-to-end points of chains connecting junctions are considered fixed. Subject to these constraints the chains themselves continue to be unaffected by neighboring chains and remain phantom-like. As Kloczkowski et al. observe,[5] an affine network is equivalent to a phantom network with infinite junction functionality. An intermediate proposal by Flory,[6] the so-called "constrained-junction" theory, seeks to confine the fluctuations in the length of the junction–junction vector by a parameter κ. For the phantom network $\kappa = 0$, while for $\kappa = \infty$ fluctuations are totally suppressed and we recover the affine system. The extent to which these devices even partially incorporate the molecular interactions operating within the network is far from clear, not to mention the topological restriction to treelike networks incorporating no cyclic loops, which appears necessary for an analytical description of all three network models to proceed.

Early representations by Flory and by Ronca[6] were essentially phenomenological or semiempirical and limit the role of chain–chain interactions to that of restricting fluctuations in network junctions.[15] This viewpoint has been challenged by a number of workers[16] who maintain that chain–chain interactions are also present along the chain contour: entanglements along chain contours have been modeled as confining tubes,[17] loops,[18] or slipping links.[19] Real networks are, of course, entangled, and both chemical cross-linking and chain slipping must feature in any adequate description of network deformation. Characterization of polystyrene networks by small-angle neutron scattering seems to suggest disagreement with the classical theory of elasticity concerning the Gaussian distribution of chain ends, although the concept of affine deformation appears confirmed to a good approximation.[13] Non-Gaussian representations have been reviewed in detail by Treloar.[14]

In the following sections we present an analysis of the mechanical properties of polymeric elastomers formed from molecules having a monodisperse molecular weight distribution N_s between chemical cross-linkages and/or entanglements: the calculations are based upon the iterative convolution (IC) description. This powerful approach explicitly incorporates molecular interaction in a statistical mechanical treatment in which the objective is the prediction of the spatial intersegmental and junction–junction correlation functions. On the basis of such a knowledge all the principal configurational and thermodynamic properties may be readily determined, together with the associated scattering functions which arise in the direct experimental investigations of the structure of the system. The IC technique has been applied to a wide range of polymeric systems, including linear chains, rings, stars, ladders, knots, and polynematic sequences, not to mention boundary phenomena—development of loops, trains, and tails and the calculation of segment density distributions normal to the boundary. While the majority of the calculations have been performed for hard-sphere segmental interactions, there is no a priori reason why more realistic interactions should not be adopted, nor need

0024-9297/92/2225-1604$03.00/0

the systems be compositionally homogeneous. However, for the purposes of simplicity and to explicitly identify the role of excluded volume processes in the configurational properties of such systems, we generally restrict ourselves to hard-sphere, homogeneous assemblies which, incidentally, make the Monte Carlo simulations with which we compare our theoretical analyses considerably more amenable. It is on the basis of these comparisons that we conclude that the IC approach provides a sound basis for the description of the configurational properties of self-interacting polymers, and we apply it here with confidence.

The motivation for the incorporation of molecular details of the network derives from the increasing demand for the development of polymeric products, such as elastomers, having specific and desirable physical properties. For example, Mark et al.[7] have recently investigated cross-linked networks made of blends of very short and very long PDMS chains. These bimodal networks appear to show synergism in their elastical properties coupled with high tenacity values which do not appear to follow the expected "weight-average" rule. Such systems have recently been the subject of computer simulation,[8] and clearly their description is beyond the scope of the phantom network theory and its derivatives.

As we have already mentioned, the iterative convolution technique has been applied to a wide variety of systems, in particular stars.[9] Star polymers were modeled as a central hard-sphere vertex particle to which were attached f identical branches of N_s hard-sphere segments: the molecular weight of the system was therefore $N = fN_s + 1$. The normalized intersegmental spatial correlations $Z(r_{ij}|N)$ between any pair of monomers i,j within the N-mer were determined in the IC approximation as a function of branch length and functionality f. As in all the analyses based upon the IC approximation, a knowledge of the complete set of correlation functions and their moments within the system provides a powerful approach to quantities such as the segment density profile, the mean square length, and the radius of gyration, not to mention the associated particle scattering function, $P(k)$. Here we model the network as a dilute system of coupled stars (Figure 1a) with the branches representing the flexible chains linking the junctions in the network and the vertex particles representing the junctions. The functionality of the network is the functionality of the stars, although not all branches of the stars need be fully connected to neighboring junctions. Such would be the case, for example, in which cross-linkage within the system is not fully reacted: these "dangling chains" would be elastically inactive but nevertheless would continue to participate geometrically within the self-interacting network. Here, however, we investigate a fully reacted system in which all chains participate equally in the structural and mechanical properties of the network.

While the present treatment undeniably lacks the elegance and sophistication of some other analyses, it does provide a simple statistical insight into the principal processes which contribute to the mechanical properties of the network. To this extent our presentation partially complements some of the more abtruse treatments which do not always provide a ready insight into the processes operating within the network, and this limited objective should be understood from the outset. Nevertheless, we remind the reader that the present description explicitly includes noncovalent (excluded volume) effects and is based upon a unified description of polymeric systems in terms of the spatial correlation functions $Z(r_{ij})$ between each segment pair i,j within the network.

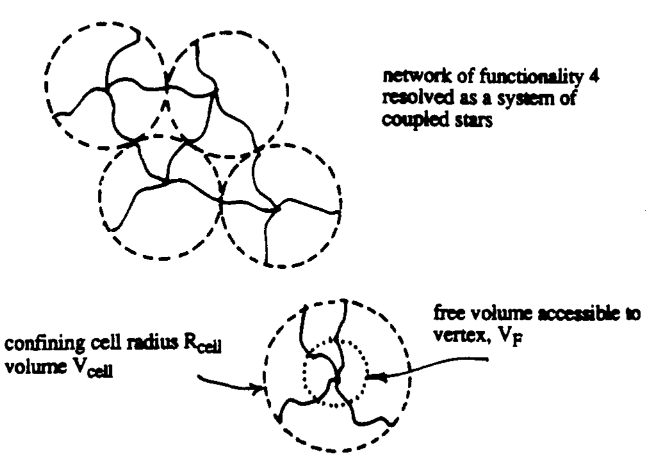

Figure 1. (a, Top) Two-dimensional representation of the network topology resolved as a system of coupled stars. The star vertex represents the point of chemical cross-linkage, while the branches represent the chain linking the junctions. The chains are modeled as sequences of self-avoiding hard-sphere segments. (b, Bottom) Confining cell, radius R_{cell}, within which the star is occluded. It is assumed that, throughout the range of network compression and expansion investigated, each star remains fully occluded within R_{cell}. The presence of the surrounding network is indicated by terminal attachment of each branch to the surface of the occluding cell. The free volume V_F accessible to the network junction (star vertex) is schematically indicated. Clearly, V_F will be sensitively dependent upon the segment diameter σ, branch length N_s, and V_{cell}.

The basis of the present analysis is strictly one of simplicity: we specifically investigate the application of simple techniques to the description of polymer networks. No suggestion is implied or intended that this iterative convolution description of coupled stars represents any more than a simple approach to the mechanical and scattering properties of the network. In fact, a systematic refinement of the present theory based, for example, on Graessley's[2] micronetwork description or even a combination with the phantom theory of networks might yield some further improvement.[24] Hence, however, we intentionally restrict ourselves to the present simplistic approach with no aspiration, intended or otherwise, to any systematic refinement. However, we do agree with the reviewer[24] that the IC treatment presented here may well form the basis of a more systematic study based on the micronetwork or the phantom network descriptions.

The Model

As briefly outlined above, we model the isotropic network as a coupled system of three-dimensional self-avoiding stars of functionality f, which may or may not be fully connected depending upon the degree of completion of the cross-linkage reaction. Star vertices are identified as junctions in the network, while chains linking junctions are the star branches (Figure 1a). The stars are regarded as being somewhat spatially constrained by virtue of their connectivity to the rest of the network, and accordingly we regard the vertex particle (or junction) and connecting branches as being occluded within a hypothetical surrounding spherical cell with the terminal segment of each branch being obliged to reside on the surface of the confining cell (Figure 1a). We note in passing that in specifying the branch length as N_s segments within each cell, we imply that the contour length of chain between junctions in adjacent cells is $2N_s$ segments. We also draw attention to the important simplification in this model whereby chains in adjacent cells of the network are not *sequentially* connected, enabling an assumption of statistical decoupling between adjacent stars to be made. Nevertheless, the cells *are* mechanically connected in that the branches are tethered to the surface of the occluding cell.

As in most other treatments, polydispersity in chain length between junctions and junction functionality is not taken into account. However, Higgs and Ball[22] have recently used the random resistor network analogy to account for the polydispersity in chain length between junctions, although in the context of the phantom network. The present approach allows us to express the total partition function for the system, Z_N, as the product z^N of the N individual star systems constituting the network for the purposes of calculating the statistical thermodynamic properties of the system. This is, of course, no more than an application of the cell theory of liquids, although with rather more of a justification in the case of a network. Thus, the total configurational energy of the network when all the junctions are centered within their cells is

$$u_0 = N\epsilon_0/2 \tag{1}$$

while if $\epsilon(\mathbf{r}_i)$ designates the cell potential developed within a cell as the ith junction wanders away from its central position, then

$$\mathbf{u} = N\epsilon_0/2 + \sum_i \epsilon(\mathbf{r}_i) \tag{2}$$

It should be appreciated that $\epsilon(\mathbf{r}_i)$ embodies the total energy of self-interaction of each star within its cell. As usual, the factor of $^1/_2$ assumes that ϵ_0 is the sum of mutual pair energies of one "star" with all the others. The coordinates $\mathbf{r}_1$, $\mathbf{r}_2$, ..., etc. are confined to cell 1, 2, ..., respectively, so that no part of any star wanders outside its confining cell. The configurational integral for the N cells then becomes[10]

$$Z_N = \exp(-N\epsilon_0/2kT)\int\!\!...\!\int \exp(-\sum_i \epsilon(\mathbf{r}_i)/kT)\,\mathrm{d}\mathbf{r}_1...\mathrm{d}\mathbf{r}_N \tag{3}$$

By specifying $\mathbf{r}_i$, the radial location of the ith junction from the center of its confining cell, to be the coordinate determining $\epsilon(\mathbf{r}_i)$, we are assuming spherical symmetry in the undeformed network. Under these circumstances and assuming no correlation between cells, we are able to decouple the total partition function as follows:

$$Z_N = z^N \tag{4}$$

where z is the cell configurational integral

$$z = \exp(-\epsilon_0/2kT)\int_V \exp(-\epsilon(\mathbf{r})/kT)(4\pi r^2)\,\mathrm{d}r \tag{5}$$

and where V is the cell volume. For a hard-sphere system such as that described here, $\epsilon_0 = 0$ and the integral amounts to V_F, the volume accessible to the vertex junction within the cell (Figure 1b). Clearly this quantity depends sensitively upon the size V of the confining cell, the length of the branches N_s, and the functionality, f. Remembering that the termini of the star branches are tethered to the surface of the hypothetical confining cell, we see that V_F vanishes as the cell expands, pulling the branches tight and progressively confining the spatial fluctuations of the central junction. Conversely, as the cell becomes smaller, V_F will at first increase but ultimately will become geometrically confined by the presence of the surrounding excluded volume associated with the star branches and the associated geometrical packing of the hard-sphere segments in the collapsed network.

It would be fair to say that the cell theory of liquids is generally regarded as affording little more than a primitive description of the thermodynamic properties of liquids because of the unrealistic confinement applied to the constituent molecules. However, it is precisely this aspect of the representation which makes its application to network theory particularly appropriate. Continuing on this basis, therefore, the statistical thermodynamic expression for the reduced tension P^* of the system follows as

$$P^* = \frac{P}{NkT} = \left(\frac{\mathrm{d}\ln z}{\mathrm{d}V}\right)_N \tag{6}$$

The equation of state relating the pressure (tension) to the isotropic compression (expansion) of the network and the determination of the associated bulk modulus then reduces to an estimate of $V_F(V)$ which we now present on the basis of the iterative convolution approximation.

The IC approximation has been fully described elsewhere,[11] and we repeat here only those details necessary for present purposes. Basically we seek to determine the complete set of normalized intersegmental spatial probability distribution functions (i.e., correlation functions) $Z(ij|N)$ ($\equiv Z(r_{ij}|N)$) developed between any pair of monomers i,j within the N-mer for a star confined within the cell. The only input to the calculation is the set of central pairwise potential functions $\Phi(ij)$ operating between each pair of monomers within the system. Clearly, heterogeneous systems may be readily described by an appropriate specification of the set of Φ-functions. Here, however, we restrict ourselves to a heterogeneous system in which all segments constituting the "star" are represented as unit hard-sphere monomers of diameter $\sigma = 1$:

$$\begin{aligned}\Phi(ij) &= 0 \quad r_{ij} > 1.0\\ &= +\infty \quad r_{ij} \le 1.0\end{aligned} \tag{7}$$

Of course, more realistic potentials could be used; however, for present purposes we consider their introduction to be unwarranted. The segments constituting the "star" are numbered sequentially from 0, representing the vertex particle, through $N = fN_s$, while the cell is regarded as a large "pseudoparticle" and is arbitrarily attributed the number "-1". Thus, $Z(0,-1)$ represents the radial spatial probability distribution of the vertex within the large confining cell. The star segments, including the vertex particle 0, 1, ..., i, ..., ... fN_s are occluded within the hypothetical cell -1 by the fictitious potential

$$\begin{aligned}\Phi(-1,i) &= 0 \quad r_{-1i} < R_c - {}^1/_2\\ &= +\infty \quad r_{-1i} \ge R_c - {}^1/_2\end{aligned}$$

where R_c is the radius of the confining cell. This ensures that all segment particles remain occluded within the cell radius R_c, enabling the statistical decoupling of localized regions of the network. Sequential connectivity is established by setting adjacent particle distributions to be covalent bond δ-functions. Thus, within a given branch

$$Z(i,i+1) = \delta(r_{i,i+1}-1) \quad (\delta = 0 \text{ if } r_{i,i+1} \ne 1) \tag{8}$$

Similarly, at the junction of the vertex particle and the first segment in each branch

$$Z(0,1) = Z(0,N_s+1) = Z(0,2N_s+1), \text{ etc.} \tag{9}$$

are represented by unit δ-functions. The termini of each of the branches are tethered to the inner surface of the occluding cell "-1" by requiring the segments which terminate each of the f branches of N_s segments to satisfy

$$Z(N_s,-1) = \delta(r_{N_s,-1} - R_c - {}^1/_2) \qquad (10)$$

These terminal segments are able to move freely over the inner surface of the occluding cell, radius R_s, while the other monomers are confined within the cell by means of a segment–cell hard-sphere potential. One further constraint operating between the terminal segments themselves is introduced to prevent "bunching" of the branches on the surface of the confining cell. Clearly, when the cell volume is such that the "star" is fully expanded and the branches are pulled tight, the terminal segments should, for a regular isotropic network, be isolated from one another and not allowed to congregate in any one region. This is a reflection of the rigid, lattice-like structure of the network in its fully expanded configuration. Accordingly, we specify a minimum distance of approach which terminal segments on the cell boundary are allowed to come to within each other. Of course this constraint needs to relax as the confining cell becomes smaller, allowing the possibility of bunching to the chains as the network is compressed, and so we adopt a simple minimum approach potential between branch termini on the surface such that

$$D \geq d \qquad (11)$$

where d is determined on simple geometrical considerations. On this basis we may now determine the correlation functions within the cell in the iterative convolution approximation. The distributions are related to the various pair potentials via the set of coupled integral equations[11]

$$Z(ij|N) = H(ij) \prod_{k \neq i,j}^{N}{}' \int Z(ik|N)\, Z(kj|N)\, \mathrm{d}\mathbf{k} \qquad (12)$$

where

$$H(ij) = \exp(-\Phi(ij)/kT)$$

A detailed description of the IC technique is not appropriate here, and we refer the reader to the earlier literature for a development of the theory and a range of applications.[9,11] However, suffice it to say that the objective of the technique is the self-consistent determination of the complete set of spatial correlation functions $Z(r_{ij}|N)$ between each pair of monomers i,j within the N-mer. The only input, apart from the sequential connectivity of the system, is the interaction potential operating between each pair of segments $\Phi(r_{ij})$. Equation 12 then expresses the development of the correlation between, say, segments i and j in the mean field of the correlations operating throughout the rest of the sequence including, of course, the hypothetical occluding segment -1.

The convolution integrals (eq 12) may be readily evaluated iteratively by fast Fourier transform techniques which, incidentally, directly yield the scattering function $P(k)$ for the system. Although all distributions (other than the δ-functions identified above) are determined in this process, we are particularly concerned here with the distribution $Z(0,-1|N)$ of the network junction within the occluding cell. Knowing this function, we may calculate its mean fluctuation radius about the center of the cell:

$$\langle r_F \rangle = 4\pi \int r_{0,-1} Z(0,-1|N) r_{0,-1}^2 \, \mathrm{d}r_{0,-1} \qquad (13)$$

whereupon

$$V_F = \frac{4\pi}{3} \langle r_F \rangle^3 \qquad (14)$$

This, of course, is the "free volume" accessible to the junction for an excluded volume system and will depend upon the functionality of the network f and the chain length $2N_s$ between junctions. The expansion or compression of the network as specified by the properties of the system then follows directly from eq 6, and we determine V_F as a function of the cell volume, V. The isothermal bulk modulus may then be determined directly as

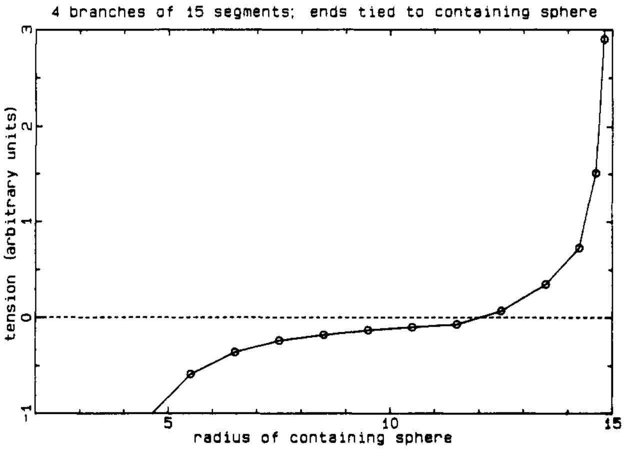

Figure 2. Bulk isotropic stress–strain relation for a hard-sphere, self-avoiding network of functionality 4 and $N_s = 15$. Note the extended linear Hookeian region in the vicinity of the unstressed network configuration ($R_{\text{cell}} \sim 12$).

$$\beta = -V(\mathrm{d}P^*/\mathrm{d}V)_T \qquad (15)$$

while its reciprocal is the compressibility of the network. Although we are primarily concerned here with the bulk modulus (or equivalently, the compressibility), there are simple relations between any given elastic constant and any two of the remaining moduli for an isotropic material. Unfortunately, however, only the bulk modulus may be determined on the basis of the present technique, and estimates of Young's modulus for a linear extension of the network would require a knowledge of, say, Poisson's ratio, not to mention a full three-dimensional treatment of the anisotropic system.

As with most previous applications of the theory, the IC technique proves to be highly versatile and may be readily extended to incorporate additional features which may characterize the network—for example, a distinction between cross-linkages and entanglements, the latter exhibiting slipping characteristics which we shall investigate further below.

It is appropriate to observe at this point that the Gaussian phantom representation and its derivatives are somewhat restricted in their application, and although they provide a useful analytic description, current interest largely centers upon the role of the various complicating molecular features of the network mentioned above: clearly these aspects are beyond the scope of the Gaussian analyses.

Results and Discussion

First we determine the athermal bulk compressibility for fully reacted, chemically cross-linked isotropic networks as a function of junction–junction chain length on the basis of the IC approximation. In Figure 2 we show the tension (compression) of the network versus volume expansion for a hard-sphere branch length of $N_s = 15$ for a fully reacted network of functionality $f = 4$. Since the system is taken to be monodisperse in the connecting sequences between junctions, the curve diverges at full network extension. In all cases there is an extended linear stress–strain region centered on the "natural" or unstressed network conformation reflecting Hookeian behavior for

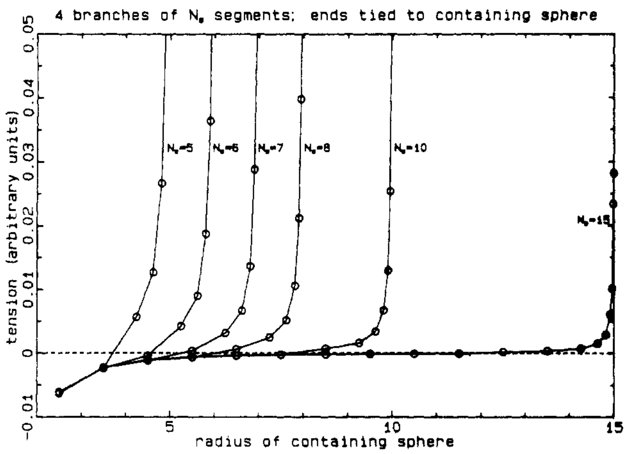

Figure 3. Stress–strain curves for the isotropic expansion of a tetrafunctional network for various chain lengths N_s.

small athermal strains of the isotropic network. The familiar cubic form of the stress–strain relationship is obtained in the limits of high compression and expansion. It should be noted that this behavior is not obtained for Gaussian networks which show an essentially linear stress–strain relation[14] and which may be directly attributed to the chain entropy term. In general, theoretical analyses do not consider the compressive branch of the curve simply because excluded volume effects begin to arise, and it is in this respect that the IC technique makes its particular contribution. For expanded networks, of course, the role of excluded volume would be expected to make a diminishing contribution, although the shortcomings implicit in the phantom network representation remain. These results are in qualitative agreement with the recent computer simulations by Termonia[8] of uniaxial and multiaxial deformation of two-dimensional networks. Termonia's analyses provide a particularly clear illustration of the microscopic processes associated with network elongation, and, without doubt, many of his conclusions may be directly extended to the case of isothermal bulk compressibility.

The stress–strain relationship for volume expansion and compression of tetrafunctional networks on the basis of the IC technique is shown in Figure 3 for various numbers N_s of hard-sphere statistical segments linking junctions. It is clearly apparent that the percentage expansion of the network necessary to achieve a given level of mechanical stress depends sensitively upon N_s, and similar conclusions have been reported by Treloar[14] for other non-Gaussian networks.

In the case of the corresponding stress–strain relationship for a network of segments having zero excluded volume ($\sigma = 0$, eq 7), we do not recover the Gaussian network result since we are restricted in this analysis to short chains linking functions which do not, of course, obey Gaussian statistics: further approximation is introduced by the IC technique. What is quite clear, however, is the coincidence of the stress–strain relationships both with ($\sigma = 1$) and without ($\sigma = 0$) excluded volume processes operating for highly expanded networks where self-avoidance plays a subordinate role and the stress–strain relationship is dominated by chain connectivity (Figure 4).

A direct comparison of our theoretical predictions of network structure may be made with SANS studies of swollen polystyrene networks, and this will be discussed below.

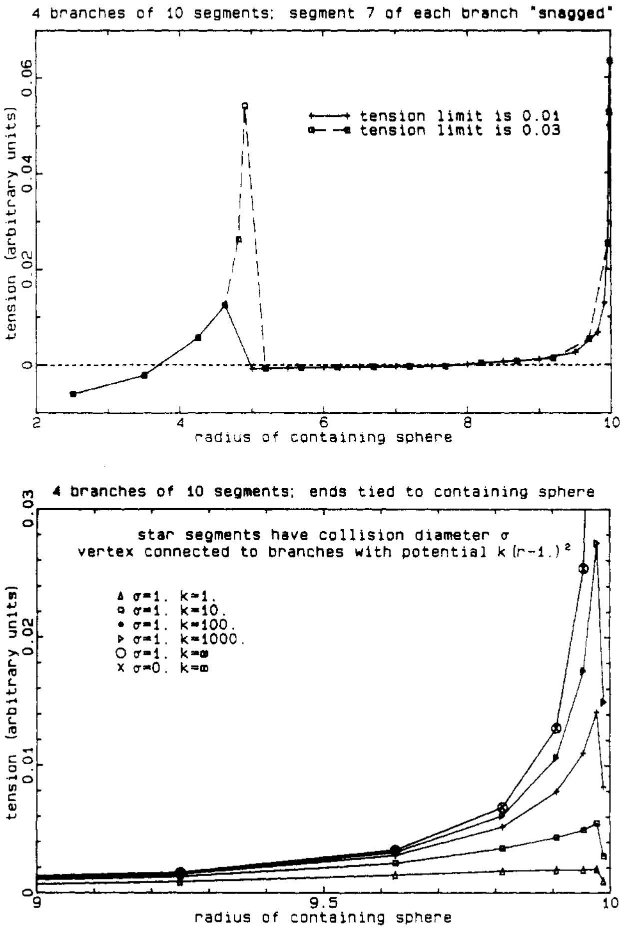

Figure 4. (a, Top) Effect of chain slippage through entanglements for two values of critical tension after which the entanglement unravels freely. (b, Bottom) Effect of chain slippage through entanglements. $k = 0$ corresponds to a disconnected network, while for $k \to \infty$ the ordinary network junctions are recovered. Also shown are the effects of excluded volume for $k = \infty$ networks. In expansion the $\sigma = 1$ and $\sigma = 0$ curves are coincident, confirming the negligible role of excluded volume for expanded networks.

Entanglement Slippage. Physical entanglements, unlike chemically cross-linked junctions, are visualized as yielding under network stress. Such behavior was explicitly incorporated in the simulations of Termonia[8] in which the nonaffine displacements of the junctions in his two-dimensional network create large force gradients on chains passing through trapped entanglements. Such gradients lead to the possibility of chain slippage which occurs in Termonia's model until the difference in force in the two strands of a chain separated by an entanglement falls below the entanglement friction force. While such processes undoubtedly occur in the equilibrium deformation of the network, Termonia maintains that the rheological behavior of the system is dominated by friction at entanglement junctions, and chain–chain interactions along the chain contour may be legitimately neglected. Certainly this proposal is sustainable for expanded networks of relatively low functionality; indeed we have already observed that the contribution of excluded volume for expanded network configurations plays a negligible role in the stress–strain relationship. However, we wish to discuss also the compression of the network in which excluded volume effects must be retained.

We model chain slippage in a similar manner to that of Termonia and regard a segment along the chain contour as being "snagged" and confined to reside within a central entangled region v. A similar approach has already been described in the iterative convolution description of knotted systems. The chains unravel freely with increasing cell size, subject of course to excluded volume and connectivity constraints, until the snagged segments reach the boundary of the central confining region. A tension limit is set within the chains beyond which the entanglement spontaneously unravels and behaves like a simple chemically cross-linked system. Of course, which segment snags and the tension limit at which slippage occurs will affect the stress–strain curves considerably, and in the absence of a detailed molecular understanding of the slippage process we can only determine the qualitative response of the network. Clearly, intensive experimental study of the network structure is warranted before a useful theoretical description can be attempted.

As we might expect, snagging of the chains at an entanglement produces an anomalous rise in tension until the tension threshold is exceeded (Figure 4a) after which the network unravels.

As we observe at various points throughout this paper, no detailed description of the molecular and entanglement structure is yet available, and to this extent proposals for the mechanism of entanglement slippage are somewhat arbitrary. Nevertheless, various possibilities may be readily incorporated in the present correlation function approach, and an alternative proposal to the "snagging" description outlined above is a harmonic model in which the branches of the network are connected to a vertex particle via a potential of the form $k(r-\sigma)^2$. Thus, $k = 0$ corresponds to a disconnected structure which can sustain no expansion, while for $k = \infty$ we recover the behavior of the fully connected network described previously. With decreasing k the network appears to be able to sustain progressively less stress for a given bulk deformation, and at large deformations the network effectively yields as the harmonic potential allows disconnection of the branches at the center of the entanglement. This is apparent from the sudden decrease in stress (Figure 4b) as the branches reach the limit of their extension.

Network Scattering. We have reviewed previously the description of polymer scattering from systems of various geometries, in particular stars, and it is inappropriate to repeat that discussion here. Instead, we restrict ourselves to those aspects of the scattering process as they relate to networks and refer the reader elsewhere for a fuller discussion.[23] Our previous analysis of polymer scattering was on the basis of the iterative convolution (IC) approximation, which is particularly suited to the calculation of scattering functions. We found that the agreement of the IC determinations ranged from good to excellent over the entire scattering domain for a wide range of macromolecular geometries, and we utilize the approach here with some confidence.

The ratio of the coherent scattering intensity $I(Q)$ to $I(0)$ at scattering vector magnitude $Q = (4\pi/\lambda)\sin(\theta/2)$ is given by the relation

$$I(Q)/I(0) = P(Q)\,S(Q) \tag{16}$$

where λ is the wavelength of the scattering radiation within the system and $P(Q)$ is the particle scattering function, in this case relating to the intrastar structure, while $S(Q)$ relates to interstar scattering. For sufficiently dilute systems $S(Q)$ may be set to unity. Here, however, star–star scattering must also be taken into account and, indeed, is an intrinsic feature of the network scattering.

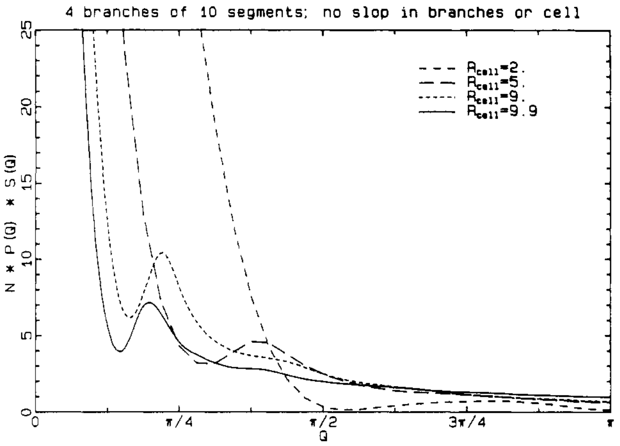

Figure 5. Scattering function (in arbitrary units) from a network of functionality $f = 4$ and branch length $N_s = 10$ determined on the basis of the IC approximation.

Both $P(Q)$ and $S(Q)$ arise as Fourier transforms of the interparticle spatial distributions on self and distinct stars, respectively. Thus, for a system of N identical point scattering centers

$$P(Q) = \frac{1}{N^2}\sum_i^N\sum_j^N \langle \exp(2\pi i\mathbf{Q}\cdot\mathbf{r}_{ij})\rangle \tag{17}$$

where $\mathbf{r}_{ij}$ is the separation of centers i,j within the molecule. Averaging over all orientations

$$P(Q) = \frac{1}{N^2}\sum_i^N\sum_j^N \left\langle \frac{\sin(Qr_{ij})}{Qr_{ij}} \right\rangle \tag{18}$$

where $\langle ... \rangle$ represents the spatial average over the scalar separation r_{ij}. These averages are nothing other than the Fourier transforms of $Z(r_{ij}|N)$, the normalized spatial probability distribution functions between centers i and j in the star determined in the course of the numerical solution of the IC integral (eq 12). In other words

$$P(Q) = \frac{1}{N^2}\sum_i^N\sum_j^N \tilde{Z}(ij|N) \tag{19}$$

where the tilde denotes the Fourier transform.

The star–star correlation from which $S(Q)$ may be determined is somewhat more difficult to evaluate. However, in the spirit of the network model adopted here we regard $S(Q)$ as the scattering from the neighboring occluding cells. These impenetrable spheres are considered as being close-packed, and their spatial distribution determined on the basis of the Percus–Yevick (PY) approximation of liquid theory. Thus, we regard the scattering from the network as arising from the stars themselves ($P(Q)$) modulated by the scattering from the occluding cells ($S(Q)$), basically, a fluid of stars occluded within their cells whose distribution is determined in the PY approximation. As the network is isotropically expanded, so the occluding cell radius increases and the star expands. The scattering product $NP(Q)\,S(Q)$ for a network of functionality 4 and branch length 10 is shown in Figure 5 for various isotropic expansions of the network. As we might expect, as the network is compressed (R_{cell} decreasing), so the scattering pattern shifts to large values of Q. This scattering behavior appears to be in good qualitative agreement with the small-angle neutron scattering experiments of Benoit et al. and Vilgis and Boué.[13] In their work scattering from polystyrene networks was determined as a function of various degrees of isotropic swelling. As in our calculations, the scattering envelope exhibits a strong diffraction maximum, the angular position of which is markedly shifted toward small angles as the swelling ratio increases. As Benoit et al. observe, a Gaussian representation of the network would yield a scattering intensity of the form $\exp(-Q^2r_{ij}^2/6)$ from a pair of scattering centers i,j, and the sum of all individual contributions will yield a steadily decreasing scattered intensity as Q increases, in which case a maximum in the scattering envelope would be impossible.

Acknowledgment. I thank Ruby Turner for performing the numerical calculations, the ARC for financial support, and the reviewer for some useful comments.

References and Notes

(1) James, H. M. *J. Chem. Phys.* **1947**, *15*, 651. James, H. M.; Guth, E. J. *J. Chem. Phys.* **1947**, *15*, 669.

(2) Graessley, W. W. *Macromolecules* **1975**, *8*, 186. Graessley, W. W. *Macromolecules* **1975**, *8*, 865.

(3) Flory, P. J. *Proc. R. Soc. London, Ser. A* **1976**, *351*, 351.

(4) Pearson, D. S. *Macromolecules* **1977**, *10*, 696.

(5) Kloczkowski, A.; Mark, J. E.; Erman, B. *Macromolecules* **1989**, *22*, 1423. Erman, B.; Kloczkowski, A.; Mark, J. E. *Macromolecules* **1989**, *22*, 1432. Kloczkowski, A.; Mark, J. E.; Erman, B. *Macromolecules* **1989**, *22*, 4502.

(6) Flory, P. J. *J. Chem. Phys.* **1977**, *66*, 5720. Ronca, G.; Allegra, G. *J. Chem. Phys.* **1975**, *63*, 4990.

(7) Mark, J. E. *Adv. Polym. Sci.* **1982**, *44*, 1.

(8) Termonia, Y. *Macromolecules* **1990**, *23*, 1481. Termonia, Y. *Macromolecules* **1991**, *24*, 1128.

(9) Croxton, C. A. *Macromolecules* **1988**, *21*, 2269.

(10) E.g.: Reed, T. M.; Gubbins, K. E. *Applied Statistical Mechanics*; McGraw-Hill, Kogakusha: Tokyo, 1973. Croxton, C. A. *Introduction to Liquid State Physics*; Wiley: London and New York, 1975.

(11) Croxton, C. A. *J. Phys. A: Math. Gen.* **1984**, *17*, 2129.

(12) Altenberger, A. R.; Dahler, J. S. *J. Chem. Phys.* **1990**, *92*, 3100.

(13) Benoit, H.; Decker, D.; Duplessix, R.; Picot, C.; Rempp, P. *J. Polym. Sci.* **1976**, *14*, 2119. Cotton, J. P.; Farnoux, B.; Jannink, G.; Mons, J.; Picot, C. *C. R. Seances Acad. Sci.* **1972**, *275*, 175. Benoit, H.; Decker, D.; Higgins, J. S.; Picot, C.; Cotton, J. P.; Farnoux, B.; Jannink, G.; Ober, R. *Nature (Phys. Sci.)* **1973**, *245*, 13. Vilgis, T.; Boué, F. *Polymer* **1986**, *27*, 1154.

(14) Treloar, L. R. G. *Rep. Prog. Phys.* **1973**, *36*, 755.

(15) Flory, P. J.; Erman, B. *Macromolecules* **1982**, *15*, 800.

(16) Langley, N. R. *Macromolecules* **1968**, *1*, 348. Ferry, J. D. *Viscoelastic Properties of Polymers*, 2nd ed.; Wiley: New York, 1979. Dossin, L. M.; Graessley, W. W. *Macromolecules* **1979**, *12*, 123. Pearson, D. S.; Graessley, W. W. *Macromolecules* **1980**, *13*, 1001. Meyers, K. O.; Bye, M. L.; Merrill, E. W. *Macromolecules* **1980**, *13*, 1045. Gottlieb, M.; Macosko, C. W.; Benjamin, G. S.; Meyers, K. O.; Merrill, E. W. *Macromolecules* **1981**, *14*, 1039.

(17) Marucci, G. *Macromolecules* **1981**, *14*, 434. Gaylord, R. J. *Polym. Bull. (Berlin)* **1983**, *9*, 181.

(18) Ball, R. C.; Doi, M.; Edwards, S. F.; Warner, M. *Polymer* **1981**, *22*, 1010.

(19) Adolf, D. *Macromolecules* **1988**, *21*, 249.

(20) Croxton, C. A. *Macromolecules*, to be published.

(21) Weiner, J. H.; Gao, J. In *Computer Simulations of Polymers*; Roe, R. J., Ed.; Prentice-Hall: Englewood Cliffs, NJ, 1991.

(22) Higgs, P. G.; Ball, R. C. *J. Phys. (Paris)* **1988**, *49*, 1785.

(23) Croxton, C. A. *Macromolecules* **1988**, *21*, 3023.

(24) I am indebted to the reviewer for these constructive suggestions as to how the present IC theory might be usefully extended.